Title

Cardiac Protein Kinase D1 ablation alters the myocytes β-adrenergic response

Authors

Mira Hernandez, Juliana

Ko, Christopher Y

Mandel, Avery R

et al.

Publication Date

2023-07-01

DOI

10.1016/j.yjmcc.2023.05.001

Peer reviewed

Published in final edited form as:

J Mol Cell Cardiol. 2023 July ; 180: 33–43. doi:10.1016/j.yjmcc.2023.05.001.

Cardiac Protein Kinase D1 ablation alters the myocytes β-adrenergic response

Juliana Mira Hernandez[a,b], **Christopher Y. Ko**[a], **Avery R. Mandel**[a], **Erin Y. Shen**[a], **Sonya Baidar**[a], **Ashley R. Christensen**[a], **Kim Hellgren**[a], **Stefano Morotti**[a], **Jody L. Martin**[a,c], **Bence Hegyi**[a], **Julie Bossuyt**[a,*], **Donald M. Bers**[a,*]

[a]Department of Pharmacology, University of California, Davis, Davis, CA 95616, United States of America

[b]Research Group in Veterinary Medicine-GIVET, School of Veterinary Medicine, University Corporation Lasallista, Caldas, Antioquia, Colombia

[c]Cardiovascular Research Institute, University of California, Davis, Davis, CA 95616, United States of America

Abstract

β-adrenergie (β-AR) signaling is essential for the adaptation of the heart to exercise and stress. Chronic stress leads to the activation of Ca^{2+}/calmodulin-dependent kinase II (CaMKII) and protein kinase D (PKD). Unlike CaMKII, the effects of PKD on excitation-contraction coupling (ECC) remain unclear. To elucidate the mechanisms of PKD-dependent ECC regulation, we used hearts from cardiac-specific PKD1 knockout (PKD1 cKO) mice and wild-type (WT) littermates. We measured calcium transients (CaT), Ca^{2+} sparks, contraction and L-type Ca^{2+} current in paced cardiomyocytes under acute β-AR stimulation with isoproterenol (ISO; 100 nM). Sarcoplasmic reticulum (SR) Ca^{2+} load was assessed by rapid caffeine (10 mM) induced Ca^{2+} release. Expression and phosphorylation of ECC proteins phospholambam (PLB), troponin I (TnI), ryanodine receptor (RyR), sarcoendoplasmic reticulum Ca^{2+} ATPase (SERCA) were evaluated by western blotting. At baseline, CaT amplitude and decay tau, Ca^{2+} spark frequency, SR Ca^{2+} load, L-type Ca^{2+} current, contractility, and expression and phosphorylation of ECC protein were all similar in PKD1 cKO vs. WT. However, PKD1 cKO cardiomyocytes presented a diminished ISO response vs. WT with less increase in CaT amplitude, slower $[Ca^{2+}]_i$ decline, lower Ca^{2+} spark rate and lower RyR phosphorylation, but with similar SR Ca^{2+} load, L-type Ca^{2+} current, contraction and phosphorylation of PLB and TnI. We infer that the presence of PKD1 allows full cardiomyocyte β-adrenergic responsiveness by allowing optimal enhancement in SR Ca^{2+} uptake and RyR sensitivity, but not altering L-type Ca^{2+} current, TnI phosphorylation or contractile response. Further studies are necessary to elucidate the specific mechanisms by which

*Corresponding authors at: Department of Pharmacology, University of California, Davis, 451 Health Sciences Drive, Davis, CA 95616, United States of America. jbossuyt@ucdavis.edu (J. Bossuyt), dmbers@ucdavis.edu (D.M. Bers).

Appendix A. Supplementary data

Supplementary data to this article can be found online at https://doi.org/10.1016/j.yjmcc.2023.05.001.

Declaration of Competing Interest

None.

PKD1 is regulating RyR sensitivity. We conclude that the presence of basal PKD1 activity in cardiac ventricular myocytes contributes to normal β-adrenergic responses in Ca^{2+} handling.

Keywords

Protein kinase D; Calcium handling; Ca^{2+} sparks; Ryanodine receptor; β-Adrenergic stimulation; EC-coupling

1. Introduction

The β-adrenergic (β-AR) signaling pathway is critical for the survival mechanism referred to as the sympathetic fight-or-flight response, but under physiological basal conditions, the sympathetic nervous system also regulates the function of several organs, including the heart. The sympathetic reflex modulates (through the β-AR pathway) the heart's response to changes in afterload by increasing heart rate and contractility [1]. This is accomplished through alterations in the activities of proteins involved in excitation-contraction coupling (ECC) including L-type Ca^{2+} channels, ryanodine receptors (RyRs), phospholamban (PLB), troponin I (TnI) and myosin binding protein C (MyBP-C) mostly by protein kinase A (PKA) [2]. In cardiac hypertrophy and failure there is chronic activation of β-AR signaling and activation of CaM kinase superfamily members such as Ca^{2+}/CaM-dependent kinase II (CaMKII) and protein kinase D (PKD) that can modulate ECC [3-6]. While CaMKII effects on ECC have been studied in detail, PKD has been less well-studied.

PKD is a serine/threonine kinase that has been strongly implicated in cardiac remodeling during, for example, pressure overload induced hypertrophy [7] and heart failure [8] and can reduce myofilament Ca^{2+} sensitivity in response to G_q-protein coupled receptor activation; e.g. endothelin-1 [4,9]. Moreover, PKD is required for the pathologic hypertrophic remodeling induced by chronic neurohumoral stimulation with isoproterenol (β-AR receptor agonist) in mice [7], indicating the interaction between PKD and the β-AR signaling pathway. However, the mechanisms by which PKD acutely modulates β-AR responses at the ECC level remain unclear. Indeed, prior studies on the molecular interaction between β-AR/PKA signaling and PKD have produced conflicting results: Harrison et al. [10] detected no effect on PKD target phosphorylation after β-AR or PKA stimulation; Carnegie et al. [11] showed that A-kinase-anchoring protein-Lbc (AKAP-Lbc) operates as a scaffold for PKA and protein kinase C (PKC) enabling PKD activation and histone deacetylase 5 (HDAC5) phosphorylation; and Haworth et al. [12] found that PKA inhibits PKD activation by endothelin-1 (ET-1) or phenylephrine (PE) and this is mediated by phosphodiesterase 3 and 4 (PDE 3 and 4). Nichols et al. identified that β-AR/PKA signaling triggers a novel nuclear PKD activation, while also suppressing the canonical PKC-dependent sarcolemmal PKD activation, demonstrating crosstalk between these two signaling pathways [13].

Here, we used a cardiac specific knockout of the major cardiac isoform, PKD1 (PKD1 cKO) [7], to test how PKD1 alters adult murine ventricular myocyte Ca^{2+} handling in the absence and presence of β-AR activation. These mice exhibit no prominent baseline phenotype with respect to cardiac size or function. However, cellular Ca^{2+} handling and contraction had not been assessed. We found no difference in ECC at baseline in PKD1 cKO myocyte. However,

we found a blunted β-AR response in Ca^{2+} transient amplitude and rate of $[Ca^{2+}]_i$ decline. The β-AR-induced increase in spontaneous SR Ca^{2+} release events (Ca^{2+} sparks) and RyR phosphorylation were also reduced in the PKD1 cKO mouse myocytes. No significant changes were observed in L-type Ca^{2+} current, contractility and phosphorylation of other key ECC proteins (e.g. TnI).

Our findings suggest that PKD1 may enhance cardiomyocyte responsiveness to β-adrenergic stimulation by modulating RyR sensitivity and without appreciably changing SR Ca^{2+} load, L-type Ca^{2+} current, PLB and TnI phosphorylation and contractility.

2. Methods

2.1. Animal models and cell isolation

All animal procedures were approved by the Institutional Animal Care and Use Committee at University of California, Davis (protocol #22824) in accordance with the Guide for the Care and Use of Laboratory Animals published by the US National Institutes of Health (8th edition, 2011).

Healthy adult (8–12 weeks, both sexes) C57BL/6 J (WT, Jackson Laboratory, stock No. 000664), Protein Kinase D1 cardiac specific knock-out (PKD1 cKO, obtained by crossing $PKD1^{loxP/loxP}$ mice (Jackson Laboratory, stock No.: 014181) with $PKD1^{loxP/loxP;\ \alpha\text{-MHC-Cre}}$ [7]), and wild-type (WT) littermates were used. Notably, the Olson group [7] did not detect PKD1 protein in western blots in these PKD1 cKO, noting that the 5-fold reduction of PKD1 mRNA in PKD1 cKO hearts may reflect PKD1 expression in fibroblasts, endothelial, smooth muscle, and immune cells within the heart (and there was no apparent compensatory upregulation of PKD2 or PKD3 in the PKD1 cKO hearts).

Isolated cardiomyocytes were obtained by enzymatic digestion of mouse left ventricles with 89 mg of type II collagenase (Worthington Biochemical Company, Cat#LS004177, Lot#41H21476, 290 units/mg dry weight) and 4 mg of type XIV protease (from *Streptomyces griseus*, Sigma-Aldrich, Cat#P5147, ≥3.5 units/mg powder). Briefly, heparin injected mice (400 U/kg body weight) were anesthetized with isoflurane (5% for induction and 3–3.5% for maintenance) and heart excision was performed. After aortic cannulation, hearts were perfused on constant flow Langendorff apparatus (37 °C) with 50 mL MEM (in mM: NaCl 135, KCl 4.7, KH_2PO_4 0.6, Na_2HPO_4 0.6, $MgSO_4$ 1.2, HEPES-free acid 20, taurine 30; and 10 μM Ca^{2+} with enzymes and 100% O_2, pH = 7.4) for 15–20 min. Subsequently, myocytes were disaggregated by gentle pipetting, filtered (nylon mesh) and sedimented repeatedly following step increases in Ca^{2+} (0.125, 0.25 and 0.5 mmol/L). Before experiments, myocytes are kept in normal Tyrode (NT) solution (in mM: NaCl 140, KCl 4, $MgCl_2$ 1, HEPES-Na 5, HEPES-H-free 5, glucose 5.5, $CaCl_2$ 0.5; pH = 7.4) at room temperature (22–23 °C).

2.2. Calcium imaging and contractility analysis

Isolated myocytes were indicator-loaded by incubation with Fluo-4 AM (10 μM, Invitrogen with Pluronic F-127 0.02%, Invitrogen) in NT for 30 min and then washed for 10 min in NT and allowed to de-esterify for an additional 20 min. Then CaT and diastolic events

(sparks) were measured at 0.5 Hz and 1 Hz pacing under acute β-adrenergic stimulation (isoproterenol, ISO, 100 nM, 5-min). Experiments were performed in paired cells (control and ISO on the same cell) at room temperature in NT solution with 1.8 mM Ca^{2+}. Line scan recordings were obtained using confocal microscopy (Bio-Rad Radiance 2100, 40× objective, 6 ms/line), exciting Fluo-4 AM with an Argon laser at 488 nm and collecting emission with a 500–530 nm bandpass filter. For SR Ca^{2+} load determination, rapid delivery of 10 mM caffeine was used. Diastolic [Ca^{2+}] variations (at rest and during pacing) were assessed by measurements of initial Ca^{2+} baseline (at rest), diastolic Ca^{2+} baseline (during pacing) and the ratio of diastolic/resting fluorescence after background subtraction (F/F_0). Recordings were analyzed with Image J-Fiji™ [14] and the SparkMaster plugin [15], with later data processing with our custom-made Python based software for CaT and SR Ca load and for contractility/fractional shortening (LineScanAnalyzer; https://github.com/DrHellgren/LineScanAnalyzer.git). Only recordings that showed no spontaneous Ca^{2+} waves or spontaneous CaT were included in the analysis. Matlab™ software was used to enhance contrast and scale fluorescence ranges to match background values in representative sparks traces.

2.3. Cellular electrophysiology

Freshly isolated ventricular cardiomyocytes were transferred to a measuring chamber (QR-40LP, Warner Instruments) mounted on a Leica DMI3000 B inverted microscope, and continuously perfused (2 mL/min) with a modified NT solution (K^+ was replaced with Cs^+) containing (in mM): NaCl 140, CsCl 4, $CaCl_2$ 1.8, $MgCl_2$ 1, HEPES 5, Na-HEPES 5, glucose 5.5, 4-aminopyridine 5, tetrodotoxin citrate 0.01, with pH = 7.40 (using HCl). Patch electrodes were fabricated from borosilicate glass (World Precision Instruments) having tip resistances of 2–3 MΩ when filled with a Cs-based pipette solution containing (in mM): CsCl 110, tetraethylammonium chloride 20, MgATP 5, HEPES 10, phosphocreatine disodium salt 5, calmodulin 0.0001, EGTA 10, $CaCl_2$ 3.6 (free [Ca^{2+}] = 100 nmol/L), with pH = 7.20 (using CsOH). The electrodes were connected to the input of an Axopatch 200B amplifier (Axon Instruments). Outputs from the amplifier were digitized at 50 kHz using Digidata 1332A A/D card (Axon Instruments) under software control (pClamp 10). Series resistance (on cell) was typically 3–5 MΩ and it was compensated by 85%. Experiments were discarded when the series resistance was high or increased by >20%.

Whole-cell L-type Ca^{2+} channel currents ($I_{Ca,L}$) were measured using 500 ms long voltage steps from holding potential of −80 mV to test potentials (between −40 and + 20 mV) every 5 s with a 50-ms pre-step to −40 mV to inactivate Na^+ channels. At the end of each experiment, $I_{Ca,L}$ was inhibited using 10 μM nifedipine. Ionic currents were normalized to cell capacitance, determined in each cell using short (10 ms) hyperpolarizing pulses from −10 mV to −20 mV. Cell capacitance was 148 ± 3 pF in WT (13 cells/6 animals) and 153 ± 4 pF in PKD1 cKO (15 cells/6 animals). All experiments were conducted at 21 ± 1 °C.

2.4. Inotropic stimulation and western blotting

Acute inotropic stimulation was performed in anesthetized WT and PKD1 cKO mice (90 mg/kg of ketamine and 4.5 mg/kg of xylazine, intraperitoneal, IP) with 1.5 mg/kg of isoproterenol (IP) for 15 min before hearts from these mice were rapidly excised, rinsed

with 0 Ca^{2+} NT solution, cut into 6–8 pieces and flash-frozen in liquid nitrogen. Samples were stored at −80 °C until use. Hearts were homogenized in ice-cold buffer containing (in mmol/L): NaCl 300, Tris-HCl (pH 7.4) 40, NaF 20, sodium pyrophosphate 2, MgCl2 1, EGTA 2, EDTA 2, 4% NP40, and protease and phosphatase inhibitors (EMD Millipore, set III and V, respectively). Protein concentration was assessed in heart homogenates with a Pierce™ BCA protein assay (Thermo Fisher Scientific, Cat#: 23225). Proteins were divided using Tris-Bis and Tris-HCl SDS-PAGE electrophoresis gels (4–12% Criterion XT Bio-Rad for PLB and 4–15% Criterion TGX Bio-Rad for TnI, SERCA, RyR and GAPDH) and then transferred to a 0.2 μm (PLB) or 0.45 μm (TnI, RyR and SERCA) nitrocellulose membrane that was then blocked with 5% blotting-grade blocker (Bio-Rad). Protein transfer success was checked with Ponceau staining. Blots were incubated overnight at 4 °C with primary antibodies: **PLB** (Badrilla, PLN, mAB A1, Cat#: A010–14, 1:2000, mouse), **PLB pS16** (Badrilla, Cat#: A010-12AP, 1:2000, rabbit), **TnI** (Cell signaling, Cat# 4002S, 1:2000, rabbit), **TnI pS22/23** (Abcam, EPR1059 (2), Cat#190697, 1:2000, rabbit), **RyR2** (Invitrogen-ThermoFisher, C3–33, Cat# MA3–916, 1:1000, mouse), **RyR pS2814** (Invitrogen-ThermoFisher, Cat# PA5–104558, 1:2000, rabbit), **RyR pS2808** (Invitrogen-ThermoFisher, Cat# PA5–36758, 1:1000, rabbit), **SERCA2** (Invitrogen, Cat#MA3–919, 1:2000, rabbit) and **GAPDH** (Bio-Rad, Cat# MCA4739, 1:2000, mouse). After primary antibody incubation, membranes were rinsed with TBS-Tween (TBST) and then incubated at room temperature with secondary antibodies (1:10000) for 2 h: Alexa Fluor 647 (Invitrogen, goat anti-rabbit, Cat# A32733) and Alexa Fluor 790 (Invitrogen, goat anti-mouse, Cat# A11357). Later, the blots were rinsed in TBST and then left washing in more TBST for 30 min until reading. Blots were imaged in the ChemiDoc™ MP Imaging System (Bio-Rad) and analyzed with Image Lab (Bio-Rad). Three technical replicates were prepared for each blot.

2.5. Statistical analysis

Data are presented as mean ± SEM. Data distribution (normality) was determined by D'Agostino-Pearson test. Two-tailed *t*-test and two-way ANOVA followed by post-hoc multiple comparison test (Tukey's) was used and are noted in each figure legend. When data were not normally distributed or $N < 6$, non-parametric tests were used. Differences were considered statistically significant if $P < 0.05$. Exact *P*-values are noted in figures or results section. GraphPad Prism 9 software was used for data analysis.

3. Results

3.1. Cardiomyocyte response to β-adrenergic stimulation is diminished in the absence of PKD1

To test whether baseline Ca^{2+} handling is altered by the absence of PKD1, CaT amplitude, tau decay, time to peak and durations were assessed. Fluo-4 AM loaded mouse ventricular myocytes were used to record CaTs by linescan images in confocal microscopy. No statistically significant differences at baseline were detected between the WT and PKD1 cKO mice (CaT amplitude $P = 0.52$; time constants (τ) of $[Ca^{2+}]_i$ decline $P = 0.12$). Paired to the baseline (control) measurements, β-AR effects (ISO) in CaT parameters were evaluated. As shown in Fig. 1, the responsiveness to β-AR stimulation (induced by 100

nM ISO) was diminished in the PKD1 cKO mice compared to the WT mice, with smaller CaT amplitudes and slower kinetics as indicated by longer time constants (τ) of $[Ca^{2+}]_i$ decline and CaT duration at 90% decline ($CaTD_{90}$; Fig. 1 D-F). Diastolic $[Ca^{2+}]_i$ (minimum during pacing, F/F_0) had comparable changes with respect to baseline fluorescence (at rest, non-paced, $F_0 = F_{cell}\text{-}F_{background}$) before and after ISO in both groups ($P = 0.87$; Supplemental Fig. S1A-B).

3.2. β-AR stimulation-induced increase in Ca^{2+} spark rate is reduced in PKD1 cKO cardiomyocytes

To assess whether PKD1 modulates spontaneous SR Ca^{2+} release through RyRs or SR Ca^{2+} load, Ca^{2+} spark rate and caffeine-induced CaT were measured. No significant difference in Ca^{2+} spark rate at baseline was detected between the WT and PKD1 cKO mice (means 0.128 ± 0.027 and 0.078 ± 0.009; SEM; $P = 0.81$). In both WT and PKD1 cKO myocytes, ISO induced an increase in Ca^{2+} spark frequency (CaSp frequency; Fig. 2C). However, the CaSp frequency achieved in the PKD1 cKO myocytes was significantly less than that observed in WT. The SR Ca^{2+} load at the end of the Ca^{2+} spark recording period was also not different between WT and PKD1 cKO myocytes, both before and after ISO (Fig. 2D). The apparent ISO-induced decrease in SR Ca^{2+} load could have been due to the increase in Ca^{2+} spark frequency and net Ca^{2+} extrusion via Na^+/Ca^{2+} exchanger during rest while Ca^{2+} sparks were measured. To test this possibility, we repeated the pacing protocol (in separate cells) and tested SR Ca^{2+} load immediately after stimulation was stopped, and in most cells an increase in SR Ca^{2+} load with ISO was observed (Fig. 2F). Normalizing Ca^{2+} spark frequency to these SR Ca^{2+} loads (Fig. 2G) did not change the conclusions from Fig. 2E. Despite the lower absolute CaSp frequencies in PKD1 cKO myocytes in ISO, the fold-change in response to ISO was not statistically different between the groups (Fig. 2H). That may relate to a lower basal CaSp frequency in PKD1 cKO (Fig. 2C), which was not significant, but might have contributed in part to the lesser ISO-induced Ca spark level observed in PKD1 cKO.

3.3. β-adrenergic regulation of L-type Ca^{2+} current ($I_{Ca,L}$ in PKD1 cKO ventricular myocytes is unaltered

The L-type Ca^{2+} channel is an important downstream target of the β-adrenergic signaling pathway and critically contributes to increasing CaT [16,17]. As expected, ISO markedly increased the L-type Ca^{2+} current ($I_{Ca,L}$) in WT murine ventricular myocytes (Fig. 3A-B) and induced a characteristic leftward shift in activation voltage (Fig. 3C). ISO also slightly slowed $I_{Ca,L}$ decay and enhanced $I_{Ca,L}$ recovery from inactivation in WT, whereas voltage-dependence of inactivation was unchanged (Fig. 3B-C). Importantly, in PKD1 cKO as in WT, ISO induced identical increase in $I_{Ca,L}$ density, activation voltage shift, slowing of inactivation, and enhanced recovery (Fig. 3A-C). Baseline $I_{Ca,L}$ magnitude and biophysical parameters were also indistinguishable in PKD1 cKO vs. WT. These data suggest that the impaired β-adrenergic CaT response in PKD1 cKO is not due to $I_{Ca,L}$ hypo-responsiveness. In line with this, PKD1 has already been shown to regulate L-type Ca^{2+} channel in neonatal rat cardiomyocytes; however, this regulation occurred only upon stimulation with α-adrenergic rather than β-adrenergic agonists [18].

3.4. β–AR induced changes in myocyte contractility were similar in WT and PKD1 cKO ventricular myocytes

It has been described that PKD can phosphorylate cardiac myofilaments, more specifically troponin I at serine 22/23 in mice [5]. Notably, these are the same sites that are known to be targets for the PKA-dependent phosphorylation that reduces myofilament Ca^{2+} sensitivity and contributes to faster relaxation. To determine whether the absence of PKD1 would alter baseline or ISO-induced myocyte contraction, Fig. 4 shows contraction and relaxation results in confocal images for the same cells used for CaT imaging in Fig. 1. There was a trend for more limited ISO-induced contraction amplitude ($P = 0.078$; Fig. 4B), as was seen for CaT Amplitude. However, there were no statistically significant differences in any of the contraction or relaxation parameters between the WT and PKD1 cKO ventricular myocytes either at baseline or upon β–AR stimulation. Both WT and PKD1 cKO myocytes showed an expected ISO-induced increase in contraction amplitude and rate of relaxation (Fig. 4B-C).

3.5. β–AR induced phosphorylation levels of phospholamban and cardiac troponin I were similar in both groups, whereas RyR phosphorylation was reduced in PKD1 cKO myocytes

As mentioned above, PKD monophosphorylation of serine 22/23 in cTnI was reported to be sufficient to cause marked reduction in myofilament Ca sensitivity (similar to PKA) [5,9] and that could alter ISO-induced responses. Fig. 5A-B shows that the in vivo intraperitoneal injection of ISO (1.5 mg/kg) produced robust increases in the phosphorylation of PLB at Ser16 and cTnI at Ser22/23, and these responses were similar in both WT and PKD1 cKO. Notably, there was also no difference in either expression levels or baseline phosphorylation levels of PLB or cTnI in PKD1 cKO vs. WT ($P = 0.89$ and $P = 0.58$, respectively). This suggests that under baseline conditions in WT mice, there may be insufficient PKD1 activity to significantly phosphorylate cTnI S22/23 sites. There was a slight trend toward lower PLB S16 phosphorylation in PKD1 cKO vs. WT ($P = 0.179$), which would be in the direction consistent with the slower ISO-induced $[Ca^{2+}]_i$ decline kinetics and lower CaT amplitude in the PKD1 cKO myocytes (Fig. 1D). However, no such trend was apparent in the cTnI phosphorylation data in Fig. 5B. Importantly, we found that ISO-induced RyR phosphorylation at both S2814 and S2808 sites was reduced in PKD1 cKO hearts (Fig. 5Cb-c). These data are in line with a lower RyR Ca^{2+} sensitivity and the reduced CaT amplitude and CaSp frequency observed in the PKD1 cKO myocytes (Figs. 1 and 2). The levels of RyR2 and SERCA2 expression were not different in PKD1 cKO and WT hearts ($P = 0.7$, Fig. 5Cd and Db).

4. Discussion

Protein kinases regulate a wide variety of functions in cells and are one of the largest supergene families described. In the heart, protein kinases are essential regulators of cardiomyocyte hypertrophy, protein expression and excitation-contraction coupling (ECC) modulation in physiological and pathophysiological conditions like pressure overload and heart failure [19]. Kinases also have a wide variety of intracellular distributions (compartments) and functions in the myocyte that have been described, but still there are many unknowns, and it is difficult to accurately state that a specific kinase does not have a specific function, location, or target until it is tested experimentally. Additionally, the levels

of expression and function of a kinase can vary with aging and stress stimuli or disease conditions, which all increase the complexity of the study of these proteins [19]. One of the most remarkable stimuli that alters cardiac function is the sympathetic nervous system through β-AR signaling [2]. This signaling pathway modulates ECC, protein expression and hypertrophy, and it is mediated by several protein kinases, including PKA, CaMKII and PKD (which is a member of the CaMK superfamily) [2,3,5]. Despite its key role in cardiac hypertrophy [7], PKD has been less studied in relation to ECC. In this study we tested the effects of PKD on basal ECC mechanisms and β-AR-dependent regulation of ECC in adult mouse ventricular myocytes stimulated with ISO.

Under basal physiological conditions, we did not detect any significant alteration in myocyte ECC in the absence of myocyte PKD1 expression, in terms of Ca^{2+} transient properties, contraction or $I_{Ca,L}$. These results lead us to conclude that basal PKD1 activity in the normal beating adult ventricular myocyte does not significantly alter ECC.

Activation of β-AR causes an increase in $I_{Ca,L}$, SERCA2 pump rate, CaT amplitude and kinetics, RyR-mediated Ca^{2+} spark frequency, and contraction [20]. The increases in $I_{Ca,L}$ and SERCA2 activity are expected to increase SR Ca^{2+} uptake and loading [21]. Here we showed for the first time that PKD1 ablation in cardiomyocytes blunts the response to acute β-AR stimulation (ISO) by limiting both the rise in CaT amplitude and the acceleration of CaT decay and reducing the ISO-induced increase in Ca^{2+} spark frequency (and RyR sensitivity), without significant differences in SR Ca^{2+} loading. From this we conclude that endogenous PKD1 might contribute to the enhanced cardiomyocyte response to β-AR agonists in WT adult mouse ventricular myocytes.

4.1. Mechanisms contributing to reduced β-AR responsiveness in PKD1 cKO

The first step in cardiac ECC is action potential (AP) induced activation of $I_{Ca,L}$, which is normally robustly increased in response to β-AR activation [20]. To test whether the limited CaT amplitude increase observed might be due to reduced Ca^{2+} entry via $I_{Ca,L}$, we measured $I_{Ca,L}$ in both WT and PKD1 cKO myocytes. We detected no significant differences in either baseline $I_{Ca,L}$ or its response to ISO stimulation. WT and PKD1 cKO cells both showed a nearly identical increase in $I_{Ca,L}$ density and classical shift in the I-V relationship. In both groups, ISO induced a very similar negative shift in $I_{Ca,L}$ activation voltage-dependence, no change in $I_{Ca,L}$ inactivation voltage-dependence, and slightly enhanced $I_{Ca,L}$ recovery. Some prior data suggested that PKD may modulate $I_{Ca,L}$ upon α-AR activation, which is primarily via G_q-coupled receptors that activates PKC and PKD [18,22,23]. That α-AR-induced effect was suppressed by a dominant negative PKD1 and may involve partner proteins, such as Rad-Gem/Kir-related (RGKs) and enigma homolog 1 (ENH1), but PKD has not been implicated in β-AR regulation of $I_{Ca,L}$ in the heart. We conclude that the reduced ISO-induced CaT increase in PKD1 cKO mice is not due to altered L-type Ca^{2+} channel properties in myocytes. However, the total influx of Ca^{2+} via $I_{Ca,L}$ can also be influenced by the AP duration (APD) or altered Ca^{2+}-dependent inactivation, points to be addressed later.

The next step in ECC is the $I_{Ca,L}$ triggering of SR Ca^{2+} release that is mediated by the RyR channel and the intra-SR Ca^{2+} content that is controlled by RyR, SERCA, and PLB. Of note, we found no differences in the expression levels of these three key SR proteins

in WT vs. PKD1 cKO mice, nor did we detect significant differences in SR Ca^{2+} load between WT and PKD1 cKO mice (in the absence or presence of ISO). In an effort to partially isolate RyR sensitivity as a cause of reduced ISO-induced SR Ca^{2+} release, we measured Ca^{2+} spark frequency normalized to SR Ca^{2+} load (Fig. 2E and G). We observed a similar reduction in the ISO-induced increase in Ca^{2+} spark frequency as was seen for CaT amplitude, raising the possibility that PKD1 activity might slightly increase RyR sensitivity, such that smaller SR Ca^{2+} release in the PKD1 cKO could limit the ISO-induced increase in CaTs. To test whether RyR sensitivity was altered in the PKD1 cKO mice, we assessed RyR phosphorylation at S2814 and S2808 in hearts from ISO injected mice. We found that ISO-induced RyR phosphorylation was significantly increased in WT hearts but not in PKD1 cKO hearts (Fig. 5C). Based on these weaker functional effects on Ca^{2+} handling and on RyR phosphorylation, we conclude that ISO-induced RyR sensitivity is lower in PKD1 cKO mice and this explains the smaller CaT amplitude for a given $I_{Ca,L}$ and the lower CaSp frequency in the PKD1 cKO myocytes upon ISO exposure. While the basal CaSp frequency tended toward lower values (Fig. 2C), there was no such trend in basal RyR phosphorylation in PKD1 cKO at either the S2808 or S2814 site. The trend toward lower PLB phosphorylation at baseline (Fig. 5Ab) is more in the direction that could limit basal SR Ca^{2+} content and CaSp frequency.

Whether SERCA or PLB might explain the reduced ISO-induced increase in CaT and rate of $[Ca^{2+}]_i$ decline in PKD1 cKO mice was also considered, but there were no differences in SERCA2 or PLB expression between WT and PKD1 cKO hearts and PLB phosphorylation during ISO exposure was not significantly elevated. However, there was a trend ($P = 0.179$) for a lower PLB phosphorylation ratio in PKD1 cKO hearts (basal and ISO-stimulated). While not statistically significant in the 24 hearts analyzed (6 per treatment and genotype), a slight change in that direction would agree with the lower ISO-induced acceleration of $[Ca^{2+}]_i$ decline that is a relatively direct readout of SR Ca^{2+} uptake rate, especially in mouse myocytes [21]. We conclude that a slight reduction in ISO-induced PLB phosphorylation and SR Ca^{2+} uptake rate in PKD1 cKO myocytes may explain the slower $[Ca^{2+}]_i$ decline observed in PKD1 cKO vs. WT myocytes. Such a limitation in SR Ca^{2+} uptake could also diminish SR Ca^{2+} load and so, contribute to the blunted CaT response to ISO in PKD1 cKO myocytes.

Neither resting nor diastolic $[Ca^{2+}]_i$ (during pacing) were significantly different in PKD1 cKO vs. WT myocytes (nor the ratio of diastolic/baseline Ca^{2+}; Supplemental Fig. S1). Both groups had a comparably slight change in diastolic $[Ca^{2+}]_i$ and diastolic/rest $[Ca^{2+}]_i$ ratio after ISO stimulation. Thus, we conclude that altered resting or pacing diastolic $[Ca^{2+}]_i$ are unlikely to explain the blunted ISO response in PKD1 cKO vs. WT mice.

β-AR stimulation also decreases myofilament Ca^{2+} sensitivity by PKA-dependent phosphorylation of troponin I (at S22/23). This causes a faster dissociation of Ca^{2+} from troponin C, which can speed relaxation, although this effect is more prominent when myocytes are contracting against a significant afterload [24]. In particular, in myocytes that are not mechanically tethered (as here), ISO-induced acceleration of relaxation was shown to depend entirely on PLB phosphorylation [24]. PKD shares with PKA the phosphorylation sites S22/23 on TnI [5]. Phosphorylation of these sites by PKD activation or overexpression

has been demonstrated to be sufficient to reduce myofilament Ca^{2+} sensitivity in mouse skinned trabeculae and adult ventricular myocytes (AVRM) overexpressing PKD [6]. Less phosphorylation of TnI during β-AR stimulation could also potentially alter Ca^{2+} buffering by troponin C. However, we saw no differences between the groups in TnI phosphorylation (or myocyte relaxation rates) at baseline, suggesting that PKD1 does not significantly elevate baseline cTnI phosphorylation at the regulatory S22/23 sites. The ISO-induced increases in TnI phosphorylation were also not altered in PKD1 cKO vs. WT mice, suggesting that the presence of PKD1 did not influence cTnI phosphorylation in response to ISO.

These results may not be surprising since we did not do anything to directly activate PKD (e.g., by activating G_q-coupled receptors) in either the myocytes or the intact animals. Since the phosphorylation measurements were from animals, it also suggests that endogenous PKD1 activation levels are likely quite low, even upon ISO challenge. Notably, the baseline and ISO responses for contraction and relaxation were quite similar between the groups, which largely rules out a differential change in myofilament Ca^{2+} buffering as a complicating factor for the Ca^{2+} analysis. We conclude that changes of myofilament properties in the PKD1 cKO vs. WT mice are unlikely to contribute to the reduced ISO-induced effects on myocyte Ca^{2+} transients.

The consequences of chronic β-AR activation have been extensively studied in the search for therapeutic targets that can ameliorate the deleterious changes during heart failure. Our results suggest that endogenous PKD1 has a small beneficial effect on the ability of β-AR activation to increase CaT amplitude and decay kinetics. Since PKD expression and activity are upregulated in heart failure [7,8], this potentially beneficial effect might be stronger and contribute to a degree of compensatory benefit. A potential counterpoint to that is that the more responsive β-AR effects on Ca^{2+} handling in the chronic setting could be more proarrhythmic and also drive progressive remodeling more strongly.

Our group [25] recently demonstrated that trans-aortic constriction (TAC) that induces ventricular action potential duration (APD) prolongation in WT mice was attenuated in PKD1 cKO mice. Moreover, compared to WT 8 weeks post-TAC myocytes from PKD1 cKO exhibited larger K^+ currents, including transient outward (I_{to}), sustained (I_{sus}), inward rectifier (I_{K1}), and rapid delayed rectifier K^+ current (I_{Kr}), and increased expression of corresponding K^+ channels. In TAC and sham WT myocytes, acute inhibition of PKD moderately increased I_{to} but did not alter other K^+ currents. In addition, diastolic arrhythmogenic activities were reduced in PKD1 cKO myocytes. These data suggest that PKD ablation or inhibition can attenuate some chronic arrhythmogenic effects during heart failure. Together with our data, this suggests that PKD may play a role in the attenuation of the effects during chronic β-AR activation (Ca^{2+} handling dysregulation), but further studies are required to elucidate the detailed molecular mechanisms involved.

4.2. Potential integrative mechanisms for blunted β-AR response in PKD1 cKO

The above study [25] showed that even at baseline PKD1 cKO mice have a shorter APD than WT myocytes, explained largely by a significant increase in I_{to}. The shorter APD in PKD1 cKO myocytes would limit the amount of Ca^{2+} entry via $I_{Ca,L}$ even without altering

Ca^{2+} channel expression or properties [26,27]. It would also increase the time at diastolic voltages between beats when most Ca^{2+} extrusion occurs via Na^{+}/Ca^{2+} exchange. This situation may suffice to create a slight reduction in basal myocyte and SR Ca^{2+} loading, and CaT amplitude. This may be difficult to detect statistically, but there was a mild tendency for smaller baseline CaT amplitude in PKD1 cKO vs. WT myocytes (Fig. 1D; $P = 0.081$ in unpaired *t*-test). A small difference in Ca^{2+} influx/efflux mechanisms in PKD1 cKO vs. WT could be worsened by slower baseline SERCA function, based on non-significant but slightly slower mean τ of baseline $[Ca^{2+}]_i$ decline (Fig. 1E; $P = 0.126$ in two-way ANOVA) and slightly lower baseline PLB phosphorylation (Fig. 5A; $P = 0.27$ in two-way ANOVA) and a marginally lower steady state SR Ca^{2+} content (Fig. 2F; $P = 0.156$ in unpaired t-test). So, we cannot rule out the possibility that the limited ISO-induced increases in CaT amplitude and twitch $[Ca^{2+}]_i$ decline rate (which is a readout for SERCA function, [21]) are due partly to a culmination of multiple small changes in baseline APD and SERCA function and Ca^{2+} handling coupled with small reductions in ISO-induced changes in SR Ca^{2+}-handling (via PLB and RyR properties) that limit the integrated ISO effects on CaT properties in PKD1 cKO myocytes. Prior work indicated that phosphatase (PP1) activity was slightly increased in PKD1 cKO vs. WT heart samples [28]. It is possible that such higher PP1 activity in the PKD1 cKO could also contribute to lower PLB and RyR2 phosphorylation levels upon ISO exposure, and thereby limiting the CaT amplitude, $[Ca^{2+}]_i$ decline kinetics and RyR2 desensitization (lower Ca^{2+} spark rate) in the ISO-treated PKD1 cKO myocytes.

5. Conclusion

Here we showed that PKD1-ablated cardiomyocytes have a weaker Ca^{2+} transient response to acute β-AR activation. This may be consistent with the previously demonstrated protective effect of PKD1 cKO for TAC and resistance to chronic neurohormonal stimulation in PKD1 cKO mice. In response to acute β-AR activation these PKD1 cKO myocytes have less spontaneous SR Ca^{2+} release events and a slower SERCA pump rate, without substantial compromise in overall contractility and relaxation. The molecular mechanisms by which SERCA2 and RyRs responses are blunted in PKD1 cKO mice may involve multiple small functional effects on APD and myocyte Ca^{2+} handling. Indeed, β-AR signaling involves many interacting signaling pathways and kinases (i.e. PKA and CaMKII), making this pathway complex and multifactorial. Additionally, the β-AR (specially PKA) and PKD signaling pathways have already been described to be compartmentalized within cardiac myocytes [2,13], with PKD being less well understood. Moreover, prior work has shown interaction between PKA and PKD signaling in myocytes, and the present work highlights an additional crosstalk in which PKD activity may be necessary for full PKA activation of myocyte Ca^{2+} handling upon ISO stimulation. This, of course, opens possibilities for future studies.

6. Study limitations

This study demonstrates that PKD1 ablation affects EC-coupling following β-AR stimulation in cardiac myocytes. Future studies are necessary to further elucidate the precise molecular signaling pathways that are most critical for the reduced β-AR response in

PKD1 knockout. These mechanisms, by which PKD affects EC-coupling, may modulate the integrated cardiac response in cardiac hypertrophy, heart failure, and arrhythmias, which require further investigation.

Supplementary Material

Refer to Web version on PubMed Central for supplementary material.

Acknowledgements

The authors thank all the Bers Lab members for the support with heart cells isolation, animal husbandry and general maintenance. And we thank Jakub Tomek for his contribution with the optimization of the spark representative traces.

Funding

This work was supported by grants from the Minciencias–Fulbright Colombia Scholarship (JMH), the National Institutes of Health P01-HL141084 (DMB), R01-HL142282 (DMB and JB) and R00HL138160 (SM), and Burroughs Wellcome Fund-Doris Duke Charitable Foundation “COVID-19 Fund to Retain Clinical Scientists” award (SM).

Data availability

Data are available on request from the corresponding author: Donald M. Bers – dmbers@ucdavis.edu

Abbreviations:

APD	action potential duration
β-AR	β-adrenergic
CaMKII	Ca^{2+}/calmodulin-dependent kinase II
CaSpF	calcium spark frequency
CaT	calcium transient
ECC	excitation-contraction coupling
IP	intraperitoneal
ISO	isoproterenol
NT	normal Tyrode
PKD	Protein Kinase D
PKD1 cKO	protein kinase D1 cardiac-specific knock-out
PLB	phospholamban
RyR	ryanodine receptor
SERCA	sarcoendoplasmic reticulum ATPase

SR	sarcoplasmic reticulum
TnI	troponin I
WT	wild type

References

[1]. Boron WF, Boulpaep EL, Medical Physiology, 3rd edition, Elsevier, Philadelphia, 2017.

[2]. Bers DM, Xiang YK, Zaccolo M, Whole-cell cAMP and PKA activity are epiphenomena, Nanodomain signaling matters, Physiology (Bethesda) 34 (4) (2019) 240–249.

[3]. Anderson ME, Brown JH, Bers DM, CaMKII in myocardial hypertrophy and heart failure, J. Mol. Cell. Cardiol 51 (4) (2011) 468–473. [PubMed: 21276796]

[4]. Haworth RS, Cuello F, Herron TJ, Franzen G, Kentish JC, Gautel M, Avkiran M, Protein kinase D is a novel mediator of cardiac troponin I phosphorylation and regulates myofilament function, Circ. Res 95 (11) (2004) 1091–1099. [PubMed: 15514163]

[5]. Cuello F, Bardswell SC, Haworth RS, Yin X, Lutz S, Wieland T, Mayr M, Kentish JC, Avkiran M, Protein kinase D selectively targets cardiac troponin I and regulates myofilament Ca^{2+} sensitivity in ventricular myocytes, Circ. Res 100 (6) (2007) 864–873. [PubMed: 17322173]

[6]. Martin-Garrido A, Biesiadecki BJ, Salhi HE, Shaifta Y, Dos Remedios CG, Ayaz-Guner S, Cai W, Ge Y, Avkiran M, Kentish JC, Monophosphorylation of cardiac troponin-I at Ser-23/24 is sufficient to regulate cardiac myofibrillar Ca^{2+} sensitivity and calpain-induced proteolysis, J. Biol. Chem 293 (22) (2018) 8588–8599. [PubMed: 29669813]

[7]. Fielitz J, Kim MS, Shelton JM, Qi X, Hill JA, Richardson JA, Bassel-Duby R, Olson EN, Requirement of protein kinase D1 for pathological cardiac remodeling, Proc. Natl. Acad. Sci. U. S. A 105 (8) (2008) 3059–3063. [PubMed: 18287012]

[8]. Bossuyt J, Helmstadter K, Wu X, Clements-Jewery H, Haworth RS, Avkiran M, Martin JL, Pogwizd SM, Bers DM, Ca^{2+}/calmodulin-dependent protein kinase IIdelta and protein kinase D overexpression reinforce the histone deacetylase 5 redistribution in heart failure, Circ. Res 102 (6) (2008) 695–702. [PubMed: 18218981]

[9]. Bardswell SC, Cuello F, Rowland AJ, Sadayappan S, Robbins J, Gautel M, Walker JW, Kentish JC, Avkiran M, Distinct sarcomeric substrates are responsible for protein kinase D-mediated regulation of cardiac myofilament Ca^{2+} sensitivity and cross-bridge cycling, J. Biol. Chem 285 (8) (2010) 5674–5682. [PubMed: 20018870]

[10]. Harrison BC, Kim MS, van Rooij E, Plato CF, Papst PJ, Vega RB, McAnally JA, Richardson JA, Bassel-Duby R, Olson EN, McKinsey TA, Regulation of cardiac stress signaling by protein kinase D1, Mol. Cell. Biol 26 (10) (2006) 3875–3888. [PubMed: 16648482]

[11]. Carnegie GK, Smith FD, McConnachie G, Langeberg LK, Scott JD, AKAP-Lbc nucleates a protein kinase D activation scaffold, Mol. Cell 15 (6) (2004) 889–899. [PubMed: 15383279]

[12]. Haworth RS, Goss MW, Rozengurt E, Avkiran M, Expression and activity of protein kinase D/protein kinase C mu in myocardium: evidence for alpha1-adrenergic receptor- and protein kinase C-mediated regulation, J. Mol. Cell. Cardiol 32 (6) (2000) 1013–1023. [PubMed: 10888254]

[13]. Nichols CB, Chang CW, Ferrero M, Wood BM, Stein ML, Ferguson AJ, Ha D, Rigor RR, Bossuyt S, Bossuyt J, beta-adrenergic signaling inhibits Gq-dependent protein kinase D activation by preventing protein kinase D translocation, Circ. Res 114 (9) (2014) 1398–1409. [PubMed: 24643961]

[14]. Schindelin J, Arganda-Carreras I, Frise E, Kaynig V, Longair M, Pietzsch T, Preibisch S, Rueden C, Saalfeld S, Schmid B, Tinevez JY, White DJ, Hartenstein V, Eliceiri K, Tomancak P, Cardona A, Fiji: an open-source platform for biological-image analysis, Nat. Methods 9 (7) (2012) 676–682. [PubMed: 22743772]

[15]. Picht E, Zima AV, Blatter LA, Bers DM, SparkMaster: automated calcium spark analysis with ImageJ, Am. J. Phys. Cell Phys 293 (3) (2007) C1073–C1081.

[16]. Papa A, Zakharov SI, Katchman AN, Kushner JS, Chen BX, Yang L, Liu G, Jimenez AS, Eisert RJ, Bradshaw GA, Dun W, Ali SR, Rodriques A, Zhou K, Topkara V, Yang M, Morrow JP,

Tsai EJ, Karlin A, Wan E, Kalocsay M, Pitt GS, Colecraft HM, Ben-Johny M, Marx SO, Rad regulation of ca(V)1.2 channels controls cardiac fight-or-flight response, Nat. Cardiovasc. Res 1 (11) (2022) 1022–1038. [PubMed: 36424916]

[17]. Hegyi B, Morotti S, Liu C, Ginsburg KS, Bossuyt J, Belardinelli L, Izu LT, Chen-Izu Y, Banyasz T, Grandi E, Bers DM, Enhanced depolarization drive in failing rabbit ventricular myocytes: calcium-dependent and beta-adrenergic effects on late sodium, L-type calcium, and sodium-calcium exchange currents, Circ. Arrhythm. Electrophysiol 12 (3) (2019), e007061. [PubMed: 30879336]

[18]. Maturana AD, Walchli S, Iwata M, Ryser S, Van Lint J, Hoshijima M, Schlegel W, Ikeda Y, Tanizawa K, Kuroda S, Enigma homolog 1 scaffolds protein kinase D1 to regulate the activity of the cardiac L-type voltage-gated calcium channel, Cardiovasc. Res 78 (3) (2008) 458–465. [PubMed: 18296710]

[19]. Fuller SJ, Osborne SA, Leonard SJ, Hardyman MA, Vaniotis G, Allen BG, Sugden PH, Clerk A, Cardiac protein kinases: the cardiomyocyte kinome and differential kinase expression in human failing hearts, Cardiovasc. Res 108 (1) (2015) 87–98. [PubMed: 26260799]

[20]. Bers DM, Cardiac excitation-contraction coupling, Nature 415 (6868) (2002) 198–205. [PubMed: 11805843]

[21]. Bers DM, Excitation-Contraction Coupling and Cardiac Contractile Force, Springer, Netherlands, Dordrecht, 2001.

[22]. Aita Y, Kurebayashi N, Hirose S, Maturana AD, Protein kinase D regulates the human cardiac L-type voltage-gated calcium channel through serine 1884, FEBS Lett. 585 (24) (2011) 3903–3906. [PubMed: 22100296]

[23]. Jhun BS, Wang OUJ,W, Ha CH, Zhao J, Kim JY, Wong C, Dirksen RT, Lopes CMB, Jin ZG, Adrenergic signaling controls RGK-dependent trafficking of cardiac voltage-gated L-type Ca^{2+} channels through PKD1, Circ. Res 110 (1) (2012) 59–70. [PubMed: 22076634]

[24]. Li L, Desantiago J, Chu G, Kranias EG, Bers DM, Phosphorylation of phospholamban and troponin I in beta-adrenergic-induced acceleration of cardiac relaxation, Am. J. Physiol. Heart Circ. Physiol 278 (3) (2000) H769–H779. [PubMed: 10710345]

[25]. Bossuyt J, Borst JM, Verberckmoes M, Bailey LRJ, Bers DM, Hegyi B, Protein kinase D1 regulates cardiac hypertrophy, Potassium Channel remodeling, and arrhythmias in heart failure, J. Am. Heart Assoc 11 (19) (2022), e027573. [PubMed: 36172952]

[26]. Wickenden AD, Kaprielian R, Kassiri Z, Tsoporis JN, Tsushima R, Fishman GI, Backx PH, The role of action potential prolongation and altered intracellular calcium handling in the pathogenesis of heart failure, Cardiovasc. Res 37 (2) (1998) 312–323. [PubMed: 9614488]

[27]. Lebeche D, Kaprielian R, Hajjar R, Modulation of action potential duration on myocyte hypertrophic pathways, J. Mol. Cell. Cardiol 40 (5) (2006) 725–735. [PubMed: 16600293]

[28]. Verberckmoes MRL, Jackobsen BB, Bailey LRJ, Wood BM, Bossuyt J, Protein kinase D modulation of cardiac protein Phophatases, Biophys. J 114 (3) (2018).

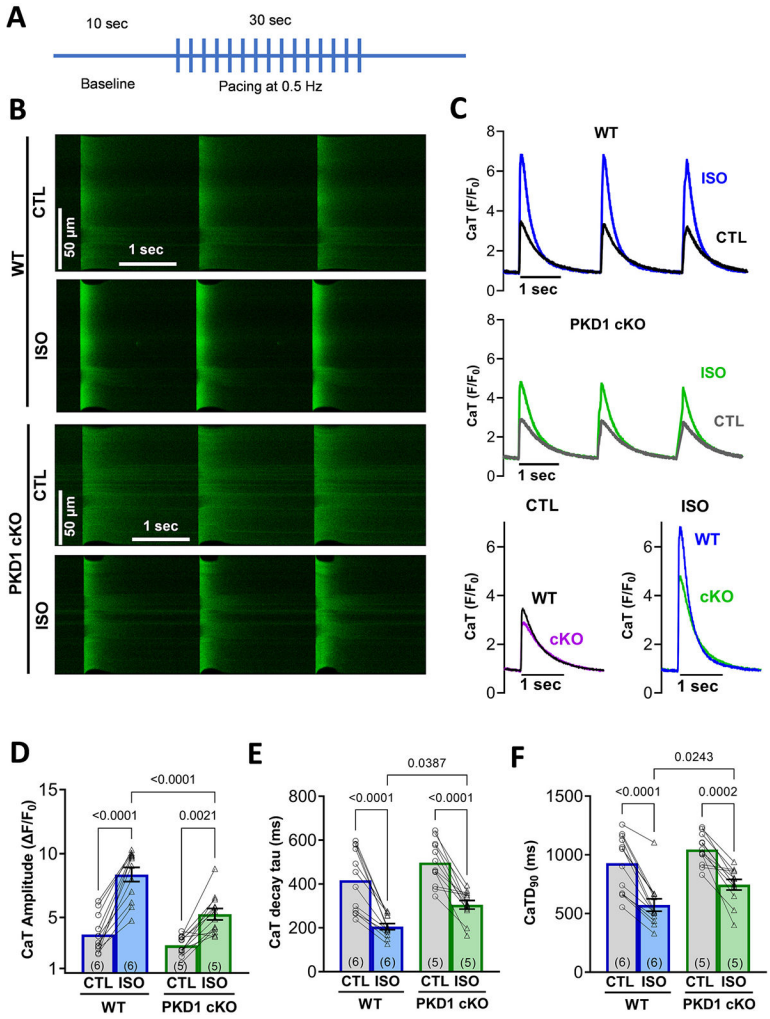

Fig. 1.

Upon acute β–AR stimulation (isoproterenol), PKD1 cKO cardiomyocytes exhibited smaller Ca^{2+} transient (CaT) amplitudes and slower kinetics compared to WT littermates. A, Experimental protocol for Ca^{2+} imaging. B, Representative confocal images and C, representative traces of intracellular Ca^{2+} transients (CaT) in both WT and PKD1 cKO Fluo-4 AM loaded myocytes at baseline and after 5-min incubation with 100 nM isoproterenol (ISO). D, CaT amplitude increase after ISO treatment was lower in the PKD1 cKO, along with slower CaT decay tau. No significant changes in CaT time to peak in both genotypes. Data points represent cells (WT, $n = 12$; KO, n = 12) and numbers on the bars the mice (WT, $N = 6$; KO, $N = 5$). Data are presented as mean ± SEM. Two-way ANOVA, followed by Tukey's multiple comparisons test. Differences were considered statistically significant if $P < 0.05$.

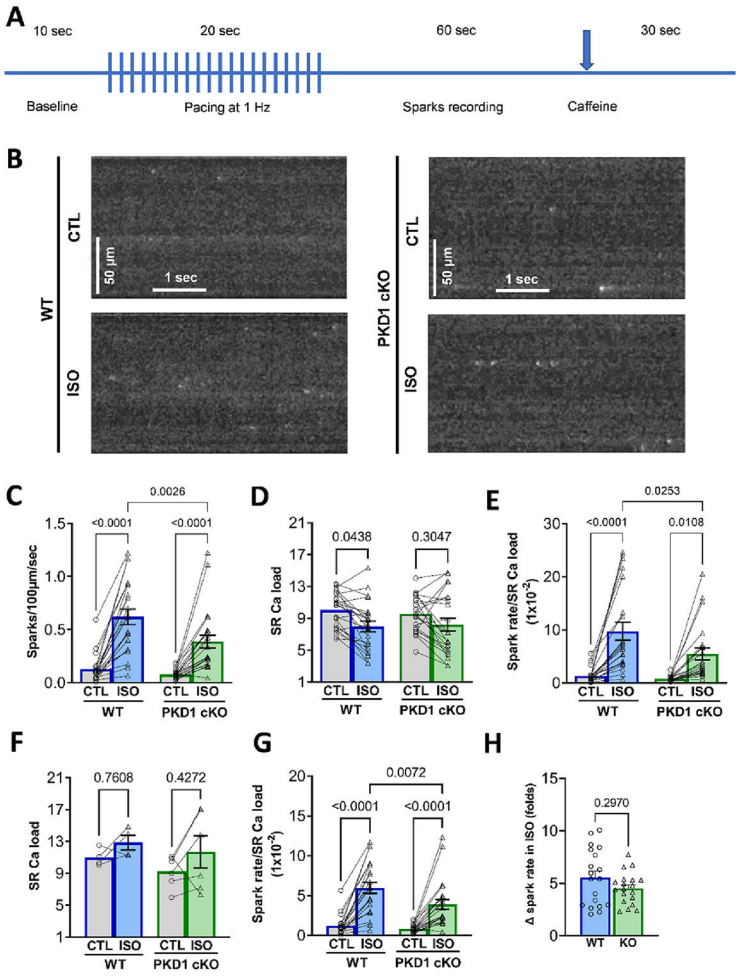

Fig. 2.

ISO-induced increase in spark rate is blunted in PKD1 cKO ventricular myocytes. A, Experimental protocol for Ca^{2+} spark measurements. B, Representative confocal images of diastolic Ca^{2+} sparks in both WT and PKD1 cKO myocytes at baseline and after 5-min incubation with 100 nM isoproterenol (ISO). Linescan image contrast was enhanced using Matlab™ software to improve visibility of Ca sparks. C, Diastolic Ca^{2+} sparks rate significantly increased more in WT myocytes. D, ISO-induced SR Ca^{2+} load decrease is similar in WT and PKD1 cKO ventricular myocytes. E, Normalization of spark rate by SR Ca^{2+} load in WT and PKD1 cKO. F, SR Ca^{2+} load measured immediately after pacing. G, Normalization of spark rate by SR Ca^{2+} load in panel F. H, Fold-change in response to ISO for Ca^{2+} spark frequency in WT and PKD1 cKO. Data points represent cells (WT, $n = 22$; KO, $n = 23$). Mice: WT, $N = 11$; KO, $N = 12$. Data are presented as mean ± SEM. Two-way ANOVA, followed by Tukey's multiple comparisons test. Differences were considered statistically significant if $P < 0.05$.

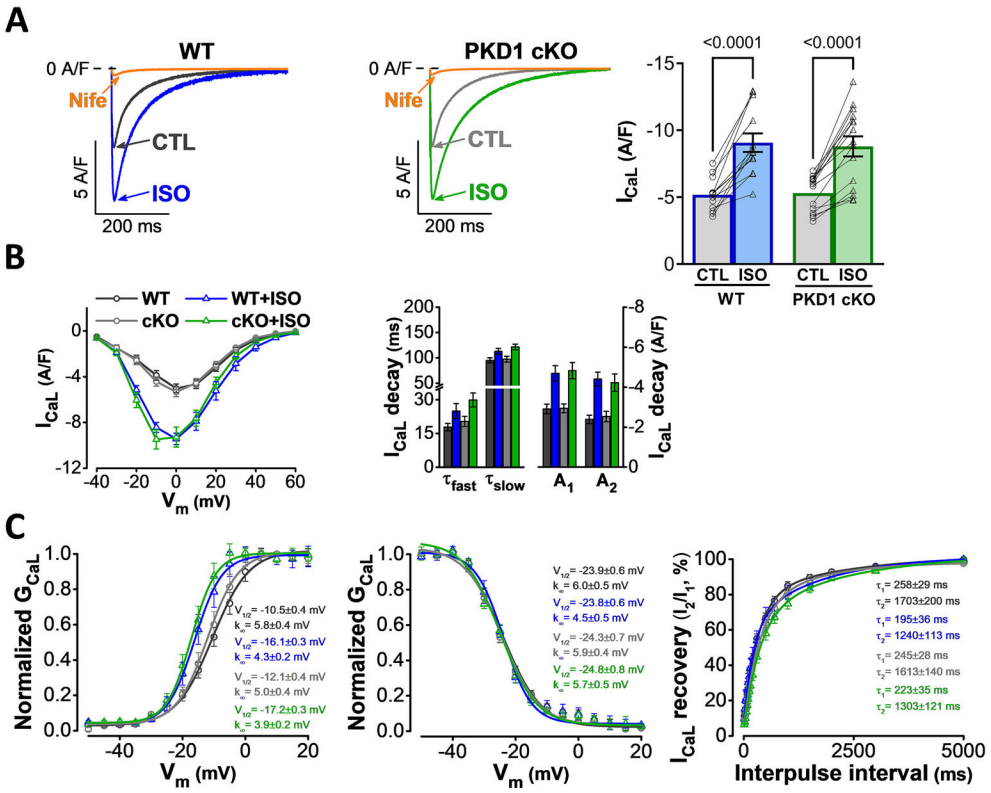

Fig. 3.

ISO-induced L-type Ca^{2+} current (I_{CaL}) increase is unaltered in PKD1 cKO ventricular myocytes. A, Representative I_{CaL} traces and average $I_{Ca,L}$ density in WT and PKD1 cKO myocytes at baseline and following 5-min treatment with 100 nM isoproterenol (ISO). Data are presented as mean ± SEM. Two-way ANOVA, followed by Tukey's multiple comparisons test. B, No difference in the ISO effect on I_{CaL} I-V relationship (left) and I_{CaL} decay (middle) between WT and PKD1 cKO. C, ISO-induced a negative shift in I_{CaL} activation voltage-dependence (left), no change in I_{CaL} inactivation voltage-dependence (middle), and slightly enhanced I_{CaL} recovery (right) in a similar way in WT and PKD1 cKO. Data were collected from 6 WT (13 cells) and 6 PKD1 cKO (15 cells) mice. Differences were considered statistically significant if $P < 0.05$.

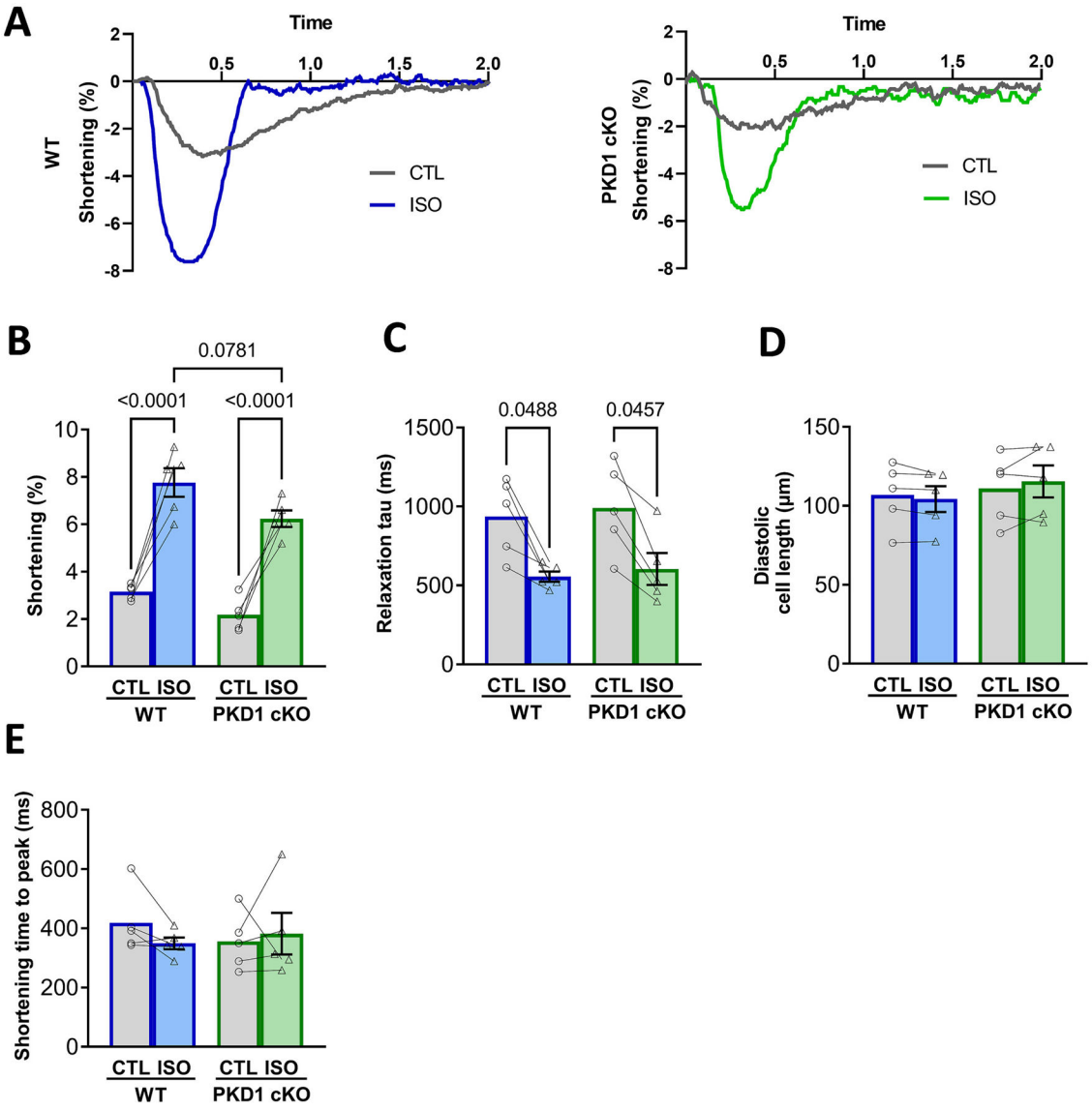

Fig. 4.

Both WT and PKD1 cKO ventricular myocytes increase contractility similarly after β–AR stimulation (isoproterenol). A, Representative traces of cell shortening in WT and PKD1 cKO myocytes. B, Fractional shortening amplitude, relaxation tau decay, time to peak of contraction and diastolic cell length were similar in both WT and PKD1 cKO myocytes at baseline and after 5-min incubation with 100 nM isoproterenol (ISO). Data points represent cells (WT, $n = 6$; KO, n = 6). Mice: WT, $N = 4$; KO, $N = 4$. Data are presented as mean ± SEM. Two-way ANOVA, followed by Tukey's multiple comparisons test. Differences were considered statistically significant if $P < 0.05$.

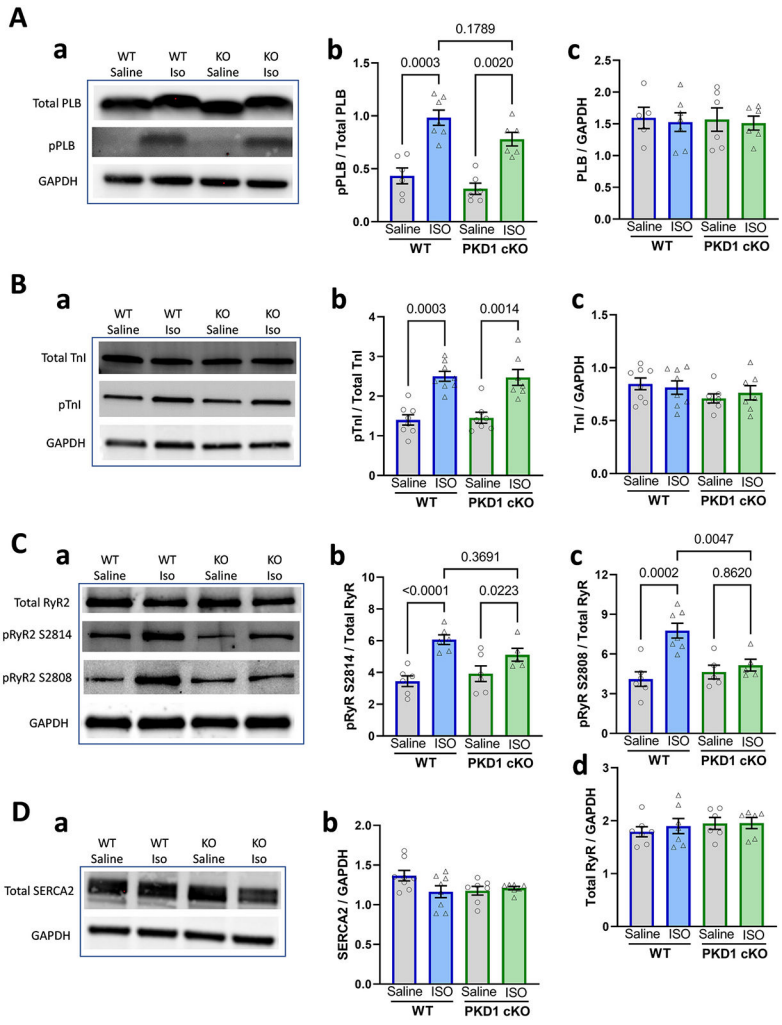

Fig. 5.

Expression and ISO-induced phosphorylation of Ca^{2+} signaling targets in WT and PKD1 cKO mice. A. Phospholamban (PLB) expression and phosphorylation at Ser16. Data points represent individual hearts (WT, *N* = 6; KO, N = 6). B. Cardiac troponin I (TnI) expression and phosphorylation at Ser 22/23 (pTnI) in representative blots (a) and pooled data (b-c). Data points are from 8 WT and 7 KO, hearts. C, RyR2 expression and phosphorylation at S2814, S2808 (pRyR) in representative blots (a) and pooled data (b-d). Data are from 7 WT and 6 KO hearts. D, Total SERCA2 expression representative blots (a) and pooled data (b) from 8 WT and 7 KO hearts. Differences were considered statistically significant if $P < 0.05$. Experiments were performed in technical triplicates for each blot. Representative blots were cropped from original full blots (included in the Supplemental data).